JOURNAL OF AIRCRAFT
Vol. 31, No. 5, Sept.–Oct. 1994

Model Ducted Propulsor Noise Characteristics at Takeoff Conditions

Richard P. Woodward*
NASA Lewis Research Center, Cleveland, Ohio 44135
Lawrence A. Bock†
Pratt & Whitney, East Hartford, Connecticut 06108
Laurence J. Heidelberg*
NASA Lewis Research Center, Cleveland, Ohio 44135
and
David G. Hall‡
NYMA Technology, Inc., Brook Park, Ohio 44142

A model Advanced Ducted Propulsor (ADP) was tested in the NASA Lewis Low-Speed Anechoic Wind Tunnel at a simulated takeoff velocity of Mach 0.2. The model was designed and manufactured by Pratt & Whitney. The 16-blade rotor ADP was tested with 22- and 40-vane stators to achieve cut-on and cut-off criterion with respect to propagation of the fundamental rotor-stator interaction tone. Additional test parameters included three inlet lengths, three nozzle sizes, two spinner configurations, and two rotor rub strip configurations. The model was tested over a range of rotor blade setting angles and inlet angles of attack. Acoustic data were taken with a sideline translating microphone probe and with a unique inlet microphone probe that identified inlet rotating acoustic modes. The beneficial acoustic effects of cut-off were clearly demonstrated. A 10-dB fundamental tone reduction was associated with the long inlet and 40-vane stator. The fundamental tone level was essentially unaffected by inlet angle of attack at rotor speeds of above 96% design.

Introduction

THE advanced propeller program[1,2] has successfully demonstrated significant performance improvements for single and counter-rotating propellers relative to that of current turbofan engines at typical cruise conditions of Mach 0.8 and 10,688-m (35,000-ft) altitude. However, uncertainties over new propeller technologies and inherent structural and acoustic benefits associated with propeller shrouds have directed current research toward the ducted propulsor, a marriage of the turbofan and propeller technologies. The ducted propulsor will typically feature a low number of rotor blades and a stator designed to satisfy the acoustic cut-off criterion.[3] Bypass ratios of 15 or greater will be characteristic of these power plants.

The objective of the present study was to quantify the aeroacoustic effects of flow parameters such as inlet length and stator vane number for a model ducted propulsor. This article will present acoustic results for a model Advanced Ducted Propeller (ADP) designed and built by Pratt & Whitney Division of United Technologies, which was tested in the NASA Lewis 9- by 15-ft Anechoic Wind Tunnel (Fig. 1a). The rotor diameter was 43.8 cm (17.25 in.). The model was tested with two different stator vane numbers (for cut-on and cut-off conditions), three inlets, two spinners, three nozzles, and with grooved and smooth rotor rub strips. A range of rotor blade setting angles was investigated. Limited diagnostic data are included from a unique rotating inlet microphone probe that allowed for separation of individual acoustic modes. Tests were conducted at Mach 0.2, which is typical of takeoff conditions.

Received June 21, 1992; revision received Jan. 3, 1994; accepted for publication Jan. 3, 1994.

*Senior Engineer. Member AIAA.
†Senior Engineer.
‡Engineer, Lewis Research Center Group. Member AIAA.

Apparatus

Anechoic Wind Tunnel

The NASA Lewis 9- by 15-ft Anechoic Wind Tunnel is located in the low-speed return leg of the supersonic 8- by 6-ft Wind Tunnel. The maximum airflow velocity in the test section is slightly over Mach 0.20, which provides a takeoff/approach test environment. The tunnel acoustic treatment provides anechoic conditions down to a frequency of 250 Hz, which is lower than the range of test propeller acoustic tones.[4]

Acoustic Instrumentation

The acoustic data presented in this article were acquired with the translating microphone probe, which is shown in Fig. 1a. This probe was instrumented with two 0.64-cm- (0.25-in.-) diam condenser microphones. Data in this report are from the outer microphone, which was located 167 cm (66 in.) from the propeller axis of rotation at 0-deg angle of attack. The probe traverse covered angles of approximately 20–140 deg relative to the propeller plane. The translating probe was programmed to travel at an approximately constant sideline angular velocity. Acoustic surveys required 180 s to complete. FFT analysis generated 52 representative sound pressure level (SPL) spectra (0–20-kHz frequency range, 32-Hz bandwidth). A computer analysis program then isolated desired tone orders (BPF, 2-BPF, etc.) to generate tone sideline directivities.

Fixed microphones were also located near the tunnel wall in the same approximate plane as the translating probe; however, data from the fixed microphones are not included in this article.

A unique rotating microphone probe was used with some configurations of the ADP model to perform a detailed investigation of inlet acoustic modes.[5] Figure 1b is a photograph showing this probe installed at the ADP inlet.

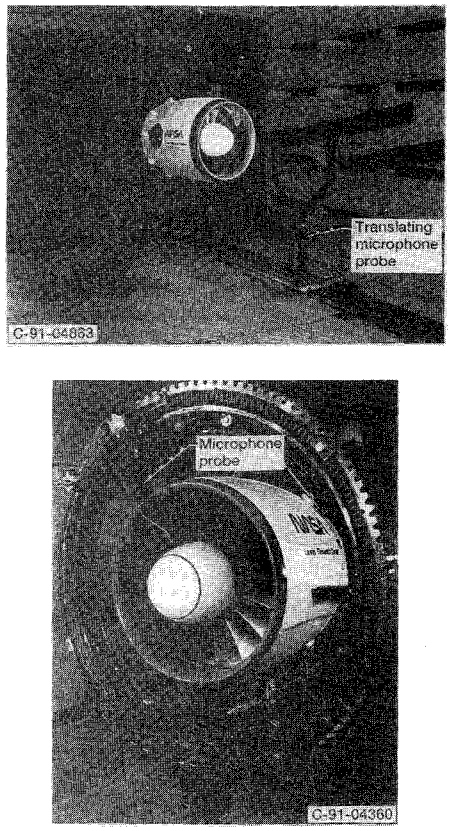

a)

b)

Fig. 1 Advanced ducted propeller acoustic installation: a) photograph of the advanced ducted propeller model installed in the 9- × 15-ft Anechoic Wind Tunnel and b) photograph of installed fan mode measurement probe.

Model Ducted Propeller

Table 1 presents design parameters for the model duct propeller. The ducted propulsor was tested with both smooth and grooved rotor rub strips. The results presented herein are for the grooved rub strip except for limited results for the smooth rub strip. The ducted propeller was powered by an air turbine drive. Exhaust air from the turbine was ducted well aft of the model and was of no aeroacoustic significance to the test results. The ADP model could be rotated in the horizontal plane to achieve inlet angle of attack. Figure 2 shows a sketch of the forward part of the model with three test inlets and two spinners.

Results and Discussion

Cut-Off Effect

Modern turbofan engines are often designed to take advantage of mode cut-off, whereby the blade passing frequency tone from rotor-stator interaction is substantially reduced in amplitude through appropriate selection of blade/vane numbers.[3] This theory predicts that the fundamental blade passage tone will be cut-off when the number of stator vanes is slightly greater than twice the number of rotor blades. The 40-vane stator satisfies this criterion for the ADP model.

Figure 3 shows representative SPL spectra for the cut-on (22-vane stator) and cut-off (40-vane stator) configurations. These spectra are for a directivity angle of 83 deg, with the rotor at 102% of design speed. The blade passing tone (BPF) is essentially in the broadband noise for the cut-off 40-vane configuration (Fig. 3a), or about 20 dB lower than that for the cut-on 22-vane stator spectrum (Fig. 3b). Other features of the spectra, such as higher-order tones and broadband, are similar for the two stator configurations.

There are reasons why the broadband noise levels were similar for the two stator configurations. The 22-vane stator had a larger aerodynamic chord than that of the 40-vane stator

Table 1 ADP design parameters

Rotor blades	16
Stator vanes	22 and 40
Rotor-stator spacing (cruise blade setting angle)[a]	
22-vane stator, chords	1.9
40-vane stator, chords	2.3
Rotor-stator spacing (takeoff blade setting angle)[b]	
22-vane stator, chords	2.2
40-vane stator, chords	2.6
Stage pressure ratio	1.243
Stage mass flow, kg/s (lbm/s)	119.9 (54.5)
Rotor diameter, cm (in.)	43.81 (17.25)
Rotor tip speed, m/s (ft/s)	257 (844)
Rotor mid-span chord, cm (in.)	7.65 (3.01)
22-vane stator midspan chord, cm (in.)	6.76 (2.66)
40-vane stator midspan chord, cm (in.)	3.73 (1.47)
Inlet dimensions[c]	
Short	
Rotor stacking line to highlight, cm (in.)	12.09 (4.76)
Highlight radius, cm (in.)	23.41 (9.22)
Throat radius, cm (in.)	21.63 (8.52)
Medium	
Rotor stacking line to highlight, cm (in.)	21.03 (8.28)
Highlight radius, cm (in.)	22.27 (8.77)
Throat radius, cm (in.)	20.43 (8.04)
Long	
Rotor stacking line to highlight, cm (in.)	26.14 (10.29)
Highlight radius, cm (in.)	21.35 (8.41)
Throat radius, cm (in.)	19.66 (7.74)
Nozzle dimensions	
Short	
Rotor stacking line to exit plane, cm (in.)	36.93 (14.54)
Exit plane radius, cm (in.)	20.45 (8.05)
Medium	
Rotor stacking line to exit plane, cm (in.)	45.27 (17.82)
Exit plane radius, cm (in.)	19.43 (7.65)
Long	
Rotor stacking line to exit plane, cm (in.)	52.26 (20.57)
Exit plane radius, cm (in.)	18.90 (7.44)

[a]Rotor midspan chord. Listed chord values are for aerodynamic chord.
[b]Cruise blade setting angle—11 deg.
[c]Fan face to rotor stacking line at cruise blade setting angle is 3.07 cm (1.21 in.).

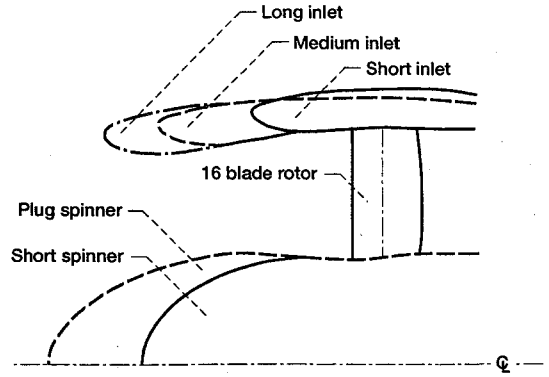

Fig. 2 ADP inlet configuration.

(see Table 1), such that the two stators had the same aerodynamic solidity. Reference 6 suggests that for this model ducted propulsor rotor-alone broadband noise is probably the dominant source of broadband noise.

Figure 4 shows corresponding BPF tone sideline directivities for the two stator configurations. The higher BPF tone levels for the 22-vane stator tend to be aft-dominant. This tendency for the BPF tone to be higher in the aft quadrant has been frequently observed for turbofans. Reference 7 suggests that acoustic blockage of the rotor-stator interaction noise attempting to propagate against the high-velocity rotor airflow is responsible for lower forward quadrant noise.

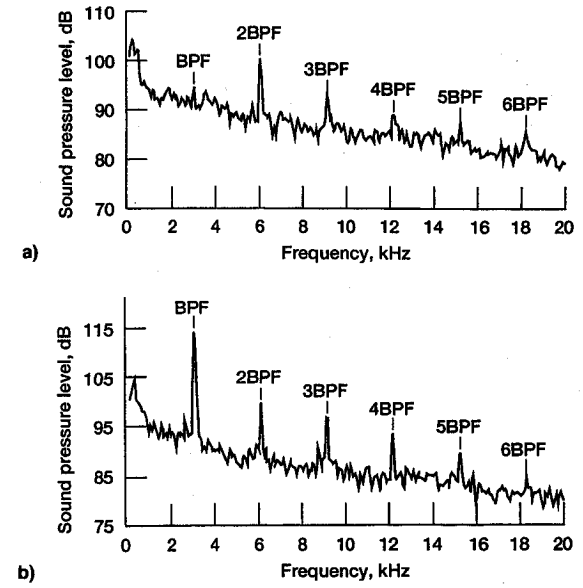

Fig. 3 Typical sound pressure level spectra for cut-on and cut-off configurations (102% design speed, long inlet, short spinner and nozzle, $\alpha = 0$ deg, $\beta = -11$ deg, $\Theta = 83$ deg, $M_\infty = 0.2$): a) 40-vane stator, cut-off and b) 22-vane stator, cut-on.

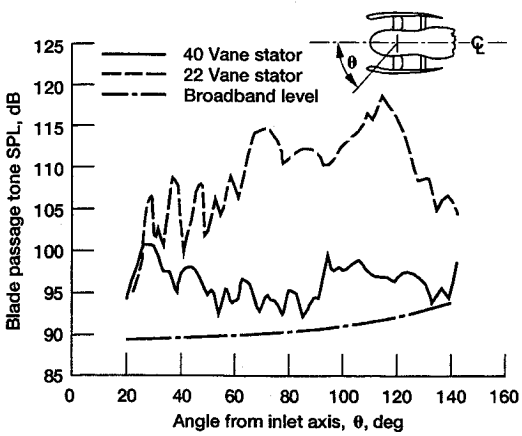

Fig. 4 Sideline BPF tone directivities for 40- and 22-vane stators (102% design speed, long inlet, short spinner and nozzle, $\alpha = 0$ deg, $\beta = -11$ deg, $M_\infty = 0.2$).

The BPF tone level for the 40-vane stator, cut-off configuration still shows some residual tone level at most directivity angles. Close inspection of the ADP model did not reveal any likely sources of inflow disturbances that might generate inflow-rotor interaction noise, with the possible exception of discontinuities in the rotor rub strip. (As will be shown in a later section of this report, the presence of the grooved rub strip did result in a somewhat higher BPF tone level at lower rotor speeds.) Reference 8 suggests that small manufacturing irregularities in the stator can result in some rotor-stator interaction tone in an otherwise cut-off fan.

Modal Analysis

A rotating microphone probe was used to provide insight into the inlet acoustic modes (Fig. 1b). The ADP model was at 0-deg angle of attack for these tests. The rake rotated at a precise fraction of the rotor speed and was synchronized with the rotor, which allowed for acoustic separation of all m order rotating circumferential modes. Five radial microphones provided some indication of the corresponding radial μ mode order, although the results presented herein are only for the outermost microphone that does not allow for definition of radial mode order.[3]

The ADP model with the rotating probe was run in both a clean inlet and a four-inlet rod configuration. The four 0.48-cm- (0.19-in.-) diam rods protruded about 25% into the flow passage and were intended to generate specific rod-rotor interaction modes. These rods were positioned 6.79 cm (2.67 in.) from the rotor stacking line plane. Circumferential mode orders m of 0, ± 4, ± 8, ± 12, etc., may be expected from this interaction, appearing at BPF in the far field. Figure 5 is a representative spectrum of the mode sound pressure levels as a function of circumferential mode number. All propagating radial mode orders μ are present in these data.

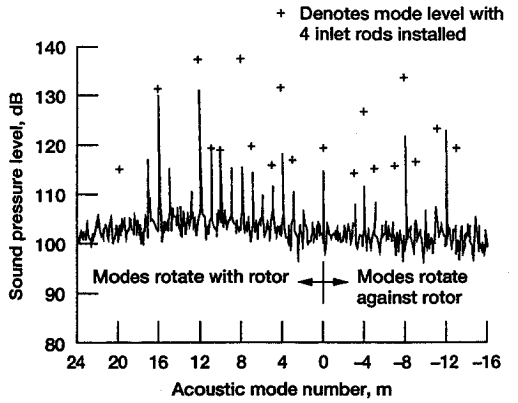

Fig. 5 Inlet acoustic mode levels (40-vane stator, 102% design speed, medium inlet, short spinner and nozzle, $\alpha = 0$ deg, $\beta = -11$ deg, $M_\infty = 0.2$).

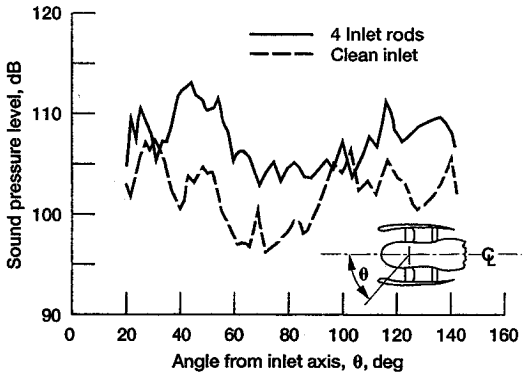

Fig. 6 Sideline directivities with and without inlet rods (BPF tone, 40-vane stator, 102% design speed, medium inlet, short spinner and nozzle, $\alpha = 0$ deg, $\beta = -11$ deg, $M_\infty = 0.2$).

The data in Fig. 5 are for 102% design rotor speed. Data are for a microphone that was 5.00 cm (1.97 in.) axially immersed from the inlet highlight, and radially 1.10 cm (0.43 in.) from the inlet flow surface. The BPF tone (3050 Hz) for the 40-vane stator configuration is predicted to be cut-off. However, there is still evidence of considerable modal activity for the clean inlet configuration. A pattern of symmetrical interruptions in the grooved rotor rub strip are thought to be the cause of this residual BPF noise. The rub strip was installed in eight sections, and a set of axial grooves was effectively missing at the junctions of these sections. Hence, there existed the possibility of an eight-lobed rotor-tip loading disturbance. Additionally, four rotor-tip proximity probes were embedded in alternate sections of the rub strip introducing the potential for a four-lobed disturbance. These disturbances are thought to be the cause for the $m = \pm 4$, ± 8, and ± 12 tones seen for the clean inlet in Fig. 5. The tone at $m = -16$ is rotating probe self-noise. Reference 5 presents a more detailed analysis of modal data that was obtained from the model ADP with this rotating inlet rake, including identification of both circumferential and radial mode orders.

Figure 6 shows BPF tone sideline directivities for the clean inlet and four-rod configurations at 102% design speed. The SPL for the inlet rod configuration is typically 10 dB or more greater than that for the clean inlet. Also, note that the maximum tone level for the inlet rod configuration occurs in the

forward quadrant rather than in the rear quadrant as was the case for the 22-vane rotor-stator interaction tone of Fig. 4. This is consistent with the concept that rod-rotor interaction noise is generated at the rotor face and is not attenuated by traversing the rotor flowfield before leaving the fan inlet.

Effect of Blade Setting Angle

This ADP model design approximated takeoff power with a rotor blade setting angle of −11 deg from the reference cruise setting angle. The model was tested over a range of blade setting angles from −7 to −18 deg, with −7 deg being the most highly loaded case with the highest mass flow.

Figure 7 shows the change in BPF SPL as a function of blade setting angle for the 40- and 22-vane stator configurations. At 86% design speed the cut-off 40-vane stator data shows little sensitivity to blade loading (Fig. 7a). A possible explanation for this observation is that the grooved rub strip reduced blade-loading sensitivity at the tip where residual rub strip—rotor interaction tone would originate. The cut-on 22-vane stator shows about a 5-dB tone level increase from −14 to −7-deg blade setting angle. This tone level is significantly greater than would be predicted by changes in thrust level [Δ dB = 10 log (thrust ratio)]. Thrust changes alone account for only 1.5 dB when the blade setting angle is changed from −7 to −18 deg. Although not predicted to be cut-on, the 40-vane stator data at 107% design speed begins to show trends similar (but significantly lower in level) to those of the 22-vane stator at 107% speed (Fig. 7b).

Figure 8 shows the corresponding maximum 2-BPF tone levels as a function of blade loading. The 2-BPF tone is cut-on for both stator configurations, although with different circumferential mode orders. At 86% speed (Fig. 8a) the 2-BPF tone increase with loading for the 22-vane stator is essentially identical to that for the BPF tone, except that the absolute levels are about 9 dB higher than those for the BPF tone. The increase in 2-BPF tone at 86% speed for the 40-vane stator over the blade loading range is about 1.5 dB, as predicted for thrust changes. The difference in 2-BPF tone level for the two stator configurations may be due to the cumulative effect of six cut-on (m, μ) tone orders for the 22-vane stator (m = 10 and −12), opposed to four m = −8 orders for the 40-vane stator. The 2-BPF tone level trends with loading are less clear at 107% design speed (Fig. 8b). However, the maximum levels for both configurations are more nearly equal with additional cut-on modal orders.

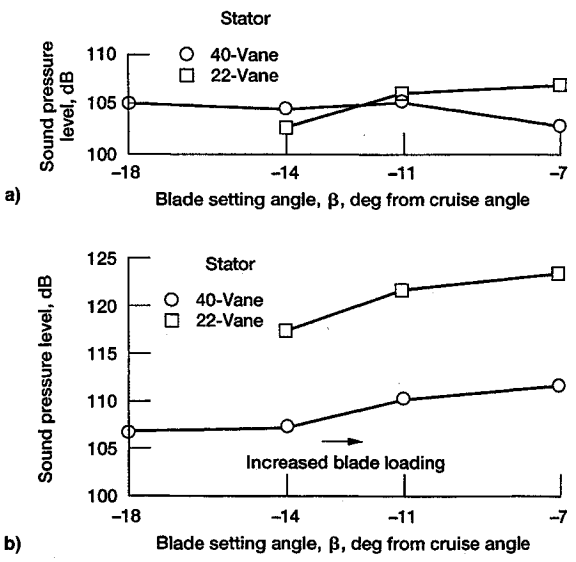

Fig. 7 Effect of blade loading on maximum sideline BPF tone level (22-vane stator with long inlet, 40-vane stator with medium inlet, short spinner and nozzle, α = 0 deg, M_∞ = 0.2): a) 86% design speed and b) 107% design speed.

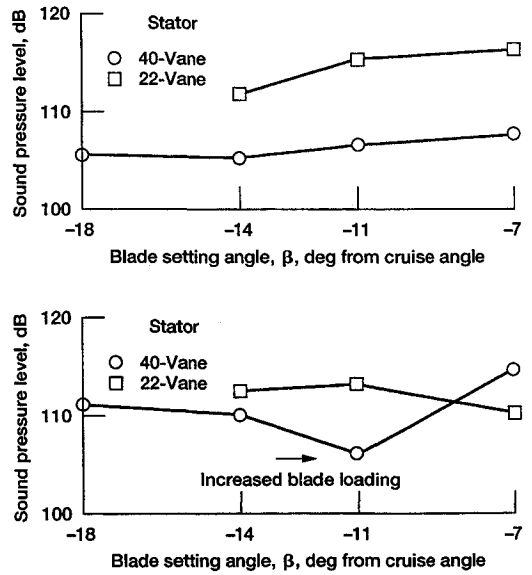

Fig. 8 Effect of blade loading on maximum sideline 2-BPF tone level (22-vane stator with long inlet, 40-vane stator with medium inlet, short spinner and nozzle, α = 0 deg, M_∞ = 0.2): a) 86% design speed and b) 107% design speed.

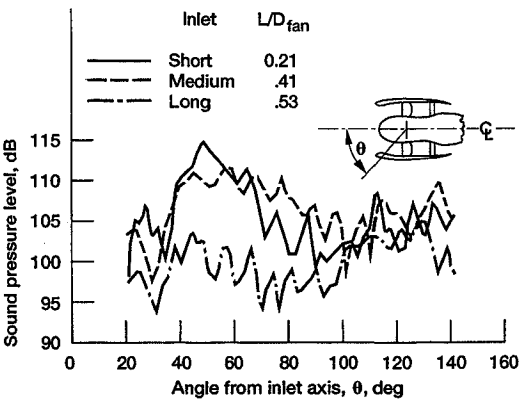

Fig. 9 Effect of inlet length on BPF tone directivity (40-vane stator, 107% design speed, short spinner and nozzle, α = 0 deg, β = −11 deg, M_∞ = 0.2).

Effect of Inlet Length

Three inlet lengths were tested. Aerodynamic performance was essentially identical for these three inlets. Figure 9 shows BPF tone directivities for the three inlet lengths with the model operating at 107% design speed. These data are for the cut-off 40-vane stator, short spinner and nozzle, and −11-deg blade setting angle. The radiated noise for the long inlet is as much as 10 dB lower than for the other two inlets in the forward quadrant. The occurrence of the highest levels in the forward quadrant are typical for rotor-inflow interaction, suggesting that in the shorter inlets unidentified inflow irregularities may be interacting with the rotor. Inspection of the overlay of the three inlet contours in Fig. 2 shows that only the long inlet extends upstream beyond the short spinner highlight, as opposed to the other two inlets that form an annulus with the spinner. Therefore, the mode release plane as well as the acoustic attenuation characteristics may be different for the long inlet.

Figure 10 extends the results of the previous figure to show the maximum forward quadrant BPF tone level for each inlet as a function of rotor speed. At BPF (Fig. 10a) there is about a 5-dB difference between levels for the long inlet and those for the other two inlets. The BPF tone levels for all inlets—and especially for the short inlet—take a sharp upward turn as the fan speed is increased to 107% design. A plot of the maximum sideline BPF tone levels for the three inlets and

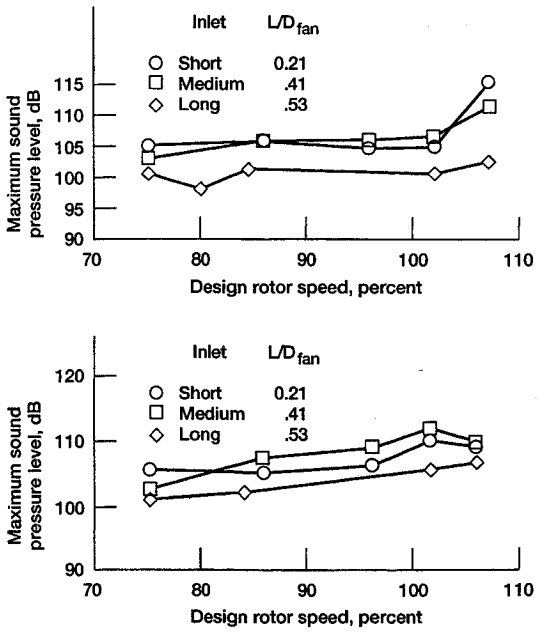

Fig. 10 Effect of inlet length on maximum forward quadrant tone level (40-vane stator, short spinner and nozzle, $\alpha = 0$ deg, $\beta = -11$ deg, $M_\infty = 0.2$): a) BPF tone and b) 2-BPF tone.

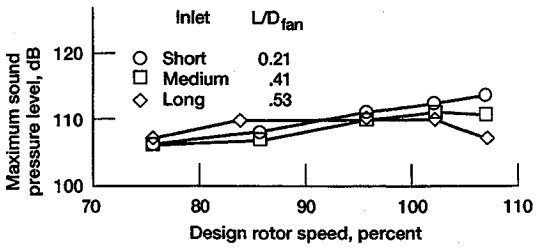

Fig. 11 Effect of inlet length on maximum sideline 2-BPF tone level (40-vane stator, short spinner and nozzle, $\alpha = 0$ deg, $\beta = -11$ deg, $M_\infty = 0.2$).

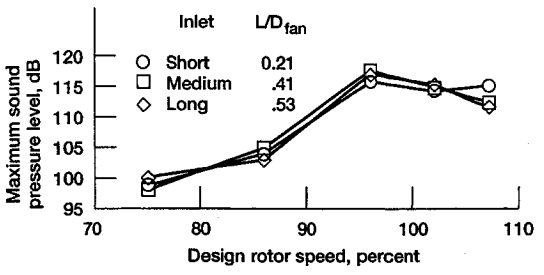

Fig. 12 Effect of inlet length on maximum forward quadrant BPF tone level (22-vane stator, short spinner and nozzle, $\alpha = 0$ deg, $\beta = -11$ deg, $M_\infty = 0.2$).

the 40-vane stator (not shown) was essentially similar, since the highest tone levels were seen in the forward quadrant for this configuration. Somewhat similar results are seen for the 2-BPF tone (Fig. 10b), where again the lowest levels are for the long inlet.

Maximum overall 2-BPF results for the three inlets and the 40-vane stator are shown in Fig. 11. The lower tone levels associated with the long inlet are only evident at the highest rotor speeds, giving further credibility that level differences in the inlet quadrant relate to different inflow-rotor interactions and/or inlet modal release dynamics.

BPF tone level differences between inlet configurations were not as significant for the 22-vane cut-on data. Directivities for the three inlet configurations with the cut-on stator were essentially similar at a particular rotor speed in contrast to those for the 40-vane stator (Fig. 9). Figure 12 shows the maximum forward quadrant BPF tone level as a function of rotor speed,

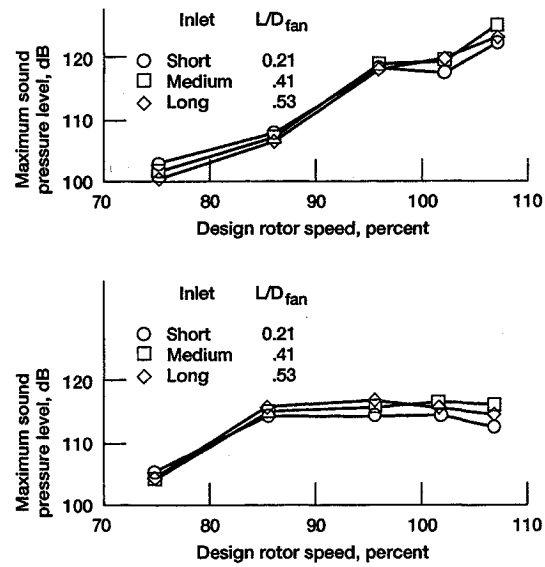

Fig. 13 Effect of inlet length on maximum sideline tone level (22-vane stator, short spinner and nozzle, $\alpha = 0$ deg, $\beta = -11$ deg, $M_\infty = 0.2$): a) BPF tone and b) 2-BPF tone.

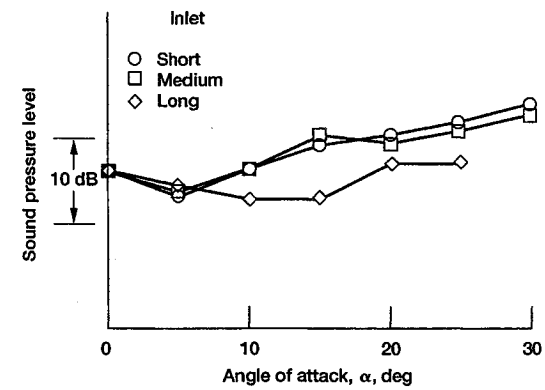

Fig. 14 Maximum sideline BPF tone level (22-vane stator, 86% design speed, short spinner and nozzle, $\beta = -11$ deg, $M_\infty = 0.2$).

whereas Fig. 13 shows similar results covering the entire sideline directivity for both BPF and 2-BPF tones. There is evidence that acoustic attenuation of rotor-stator interaction noise attempting to propagate upstream through the rotor flow becomes more significant at the higher rotor speeds (Fig. 12).

The BPF tone results for $\theta = 20$–140 deg (Fig. 13a) show an increase in level with rotor speed as would be expected for rotor-stator interaction tones, with essentially no tone level difference with inlet length. The corresponding 2-BPF results show a significant level increase between 75–86% speed, but no additional level increase with higher rotor speed. (A similar result was seen in the forward quadrant for the 2-BPF tone.) This shows that at higher speed the tonal energy for the 22-vane stator configuration is concentrated in the BPF tone (see Fig. 3).

Effect of Ducted Propeller Axis Angle of Attack

Tone level variations in the circumferential acoustic field of a free propeller operating at angle of attack has been well-documented in the literature.[9] Cyclical blade loading resulting from nonaxial inflow produces a corresponding asymmetrical circumferential noise field. A ducted propeller can be expected to exhibit increasing sensitivity to nonzero angle of attack as the duct length decreases. At 86% design speed the ADP with the 22-vane cut-on stator shows substantial BPF tone level sensitivity to inlet angle of attack for the short and midlength inlets (Fig. 14).

However, at rotor speeds above 86% design (i.e., Fig. 15) the ADP shows little acoustic sensitivity to angle of attack

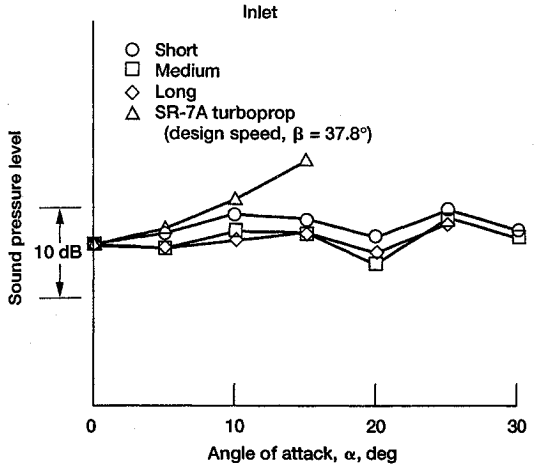

Fig. 15 Maximum sideline BPF tone level (22-vane stator, 102% design speed, short spinner and nozzle, $\beta = -11$ deg, $M_\infty = 0.2$).

regardless of inlet length. Peak BPF tone levels for a single-rotation advanced turboprop (SR-7A, Ref. 10) are superimposed on this figure, showing the unducted propeller's sensitivity to angle-of-attack effects.

Results for the 2-BPF tone (not shown) for the 22-vane stator configuration showed increasing sensitivity to inlet angle of attack with decreasing inlet length at the lowest test speed, 75% design. The 2-BPF tone was essentially unchanged with angle of attack for any inlet length at higher test speeds. The 2-BPF tone for the 40-vane stator (which was cut-on) was essentially unaffected by angle of attack for the entire range of rotor test speeds.

Effect of Spinner Type

In general, no appreciable acoustic change was associated with spinner length for the cut-off 40-vane stator. (The cut-on 22-vane stator was only tested with the short spinner.) The one minor exception to this observation was at 96% rotor speed. At this test condition there is some change in the directivity shape and level for the longer, plug spinner. The reason for this difference is unknown, although a plausible explanation may be that BPF tone noise is reflected from the longer spinner and in some manner generates a measurable interference with the directly radiating tone noise at this particular rotor speed and tone frequency.

Effect of Nozzle Length

Three nozzle configurations (see Table 1) were tested with the 40-vane stator. Aside from aerodynamic loading changes, no measurable acoustic changes were associated with nozzle type.

Effect of Rotor Rub Strip

The ADP model was tested with both smooth and grooved rotor rub strips with the cut-off, 40-vane stator. The grooved rub strip was observed to somewhat increase the stage stall margin. The grooved rub strip consisted of three circumferential rows of axial slots dimensioned approximately 1.5 by 1.5 by 12.5 mm (0.06 by 0.06 by 0.5 in.). There were 248 slots circumferentially such that rub strip-rotor interaction was clearly cut-off at blade passing frequency. However, the rub strip was installed as eight circumferential sections with one set of axial slots effectively missing at each of the eight junctions. Blade tip proximity probes were embedded in alternate rub strip sections. As will be seen, these disturbances in the rotor tip loading appear to be a tone generation mechanism for the otherwise cut-off 40-vane stator configuration.

At 75% design rotor speed and 0-deg angle of attack (Fig. 16) the maximum sideline BPF tone level with the grooved rub strip was 6 dB higher than that for the smooth rub strip. (The maximum sideline tone level was typically observed in the forward quadrant, consistent with, consistent with noise generation at the rotor.) The tone level penalty associated with the grooved rub strip decreases with increasing rotor speed, suggesting that this noise mechanism is only a factor at lower rotor speeds.

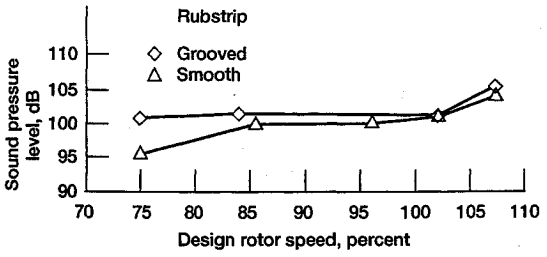

Fig. 16 Effect of rub strip type on maximum sideline BPF tone level (40-vane stator, long inlet, short spinner and nozzle, $\alpha = 0$ deg, $\beta = -11$ deg, $M_\infty = 0.2$).

Summary of Results

Acoustic tests on a model ADP were performed in the NASA Lewis 9- by 15-ft Low Speed Anechoic Wind Tunnel at a simulated takeoff flight speed of Mach 0.2. The ADP model was designed and manufactured by Pratt & Whitney Aircraft. The model was tested with three inlet lengths, three nozzle sizes, two spinner types, and two types of rotor rub strip. The model had a 16-blade rotor. Tests were made with two stator vane numbers (22 and 40) to achieve cut-on and cut-off conditions for the fundamental rotor-stator interaction tone. The model was tested over a range of rotor blade setting angles and inlet angles of attack. Acoustic data were acquired with a translating microphone probe that was attached to the tunnel floor. A unique rotating microphone probe was used to identify and measure rotating acoustic interaction modes propagating in the fan inlet. The model with the rotating probe was tested with both a clean inlet and with four rods in the inlet to generate known interaction modes.

The following significant results were observed in this study:

1) The fundamental rotor-stator interaction tone for the cut-on 22-vane stator was up to 20 dB higher than that for the cut-off 40-vane stator, with the maximum tone level occurring in the aft quadrant. This higher tone level in the aft quadrant for the 22-vane stator may be due to tone attenuation associated with propagation upstream through the rotor flowfield.

2) There was still some residual BPF tone content observed for the cut-off 40-vane stator. This residual tone was somewhat higher in the forward quadrant, and is thought to be a cut-on rotor interaction with flow over the eight-segmented rotor rub strip and four rotor tip proximity probes that were embedded in alternate rub strip sections.

3) Data from the rotating inlet acoustic probe effectively identified acoustic mode circumferential order and magnitude, including residual tones for the cut-off stator.

4) The maximum BPF tone level for the long inlet and 40-vane stator was consistently about 5 dB lower than corresponding tones for the medium and short inlets at all rotor test speeds. This may relate to the highlight of the long inlet being upstream of the spinner highlight, while the highlights for the other two inlets were in a region that formed an exit annulus with the spinner.

5) The BPF tone level was essentially unaffected by angle of attack for rotor speeds of 96% design and higher, indicating that all inlet lengths effectively conditioned the rotor inflow. However, the maximum sideline tone level in the inlet rotation plane did increase with angle of attack at 86% design rotor speed, with the short and midlength inlets being most sensitive to angle of attack.

6) The model was tested with both grooved and smooth rotor rub strips with the 40-vane stator. Irregularities in the grooved rub strip resulted in fundamental tone levels up to

6 dB higher than those of the smooth rub strip at lower rotor speeds, although the tone level difference became negligible as the rotor speed approached design.

References

[1]Hager, R. D., and Vrabel, D., "Advanced Turboprop Project," NASA SP-495, 1988.

[2]Groeneweg, J. F., and Bober, L. J., "NASA Advanced Propeller Research," NASA TM-101361, Sept. 1988.

[3]Tyler, J. M., and Sofrin, T. G., "Axial Flow Compressor Noise Studies," *Society of Automotive Engineers Transactions*, Vol. 70, 1962, pp. 309–332.

[4]Dahl, M. D., and Woodward, R. P., "Comparison Between Design and Installed Acoustic Characteristics of NASA 9- by 15-Foot Low-Speed Wind Tunnel Acoustic Treatment," NASA TP-2996, April 1990.

[5]Heidelberg, L. J., and Hall, D. G., "Acoustic Mode Measurements in the Inlet of a Model Turbofan Using a Continuously Rotating Rake," AIAA Paper 93-0598 (NASA TM-105989), Jan. 1993.

[6]Hall, D. G., and Woodward, R. P., "Noise Levels from a Model Turbofan Engine with Simulated Noise Control Measures Applied," AIAA Paper 93-4401 (NASA TM-106318), Oct. 1993.

[7]Philpot, M. G., "The Role of Rotor Blade Blockage in the Propagation of Fan Noise Interaction Tones," AIAA Paper 75-447, March 1975.

[8]Sofrin, T. G., and Mathews, D. C., "Asymmetric Stator Interaction Noise," AIAA Paper 79-0638, March 1979.

[9]Woodward, R. P., "Noise of Two High-Speed Model Counter-Rotation Propellers at Takeoff/Approach Conditions," *Journal of Aircraft*, Vol. 29, No. 4, 1992, pp. 679–685.

[10]Woodward, R. P., "Measured Noise of a Scale Model High Speed Propeller at Simulated Takeoff/Approach Conditions," AIAA Paper 87-0526 (NASA TM-88920), Jan. 1987.